Radiological and physico-chemical characterization of materials from phosphoric acid production plant to assess the workers radiological risks

J.L. Guerrero [1)], S.M. Pérez-Moreno [1)], F. Mosqueda [1)], M.J. Gázquez [2)], J.P. Bolívar [1)]*

[1)] *Department of Integrated Sciences, Center for Natural Resources, Health and Environment (RENSMA), University of Huelva, 21071, Huelva, Spain*

[2)] *Department of Applied Physics, University of Cadiz, University Marine Research Institute (INMAR) Cadiz, 11510, Spain*

***** Corresponding author. Tel.: +34 959219793; fax: +34 959 21 9467. E-mail addresses: manueljesus.gazquez@uca.es.

ABSTRACT

The industry devoted to the production of phosphoric acid by using as raw material sedimentary phosphate rock (PR) is considered as a NORM activity (Naturally Occurring Radioactive Materials), due to the high levels of U-series radionuclides contained in this ore, which are 1-2 orders of magnitude higher than those in unperturbed soils. This fact allowed us to develop a deep characterization of the raw materials, wastes, main intermediate materials, and final products obtained at a typical phosphoric acid factory. The elemental composition (major, minor and trace elements), radionuclide concentrations, grain size distribution, mineralogy and micro-structural composition were analyzed. The aim of this characterization was to obtain information for operators and maintenance personnel involved in clean-up and waste management operations.

The highest concentrations of some heavy metals and radionuclide activity concentrations were found in the “scales” (or internal incrustations)from the pipes that carry either phosphoric acid (PA) or the phosphogypsum waste (PG). The highest concentrations where found for ^{226}Ra and ^{40}K,with values up to 9 and 5 Bq g^{-1}, respectively. In addition, high concentrations of many toxic heavy metals and trace elements, such as Cd, Cr, Ni, Sr, Y, V, Zn, Th, and U, were found in some sludge samples.

The shielding effect of the containers/vessels/pipes has an essential role in the measured external dose in the intermediate products. The radiological implications of natural radionuclides with higher activity showed that, taking into account the most conservative scenario, the annual limit of 1 mSv y^{-1} is not exceeded.

Keywords: Phosphoric Acid, Phosphogypsum, Scales, Sludge, Natural Radionuclides, Heavy Metals, Radiological Risks.

1. Introduction

For the last 30 years, the scientific community has been aware of the importance of evaluating the occupational and environmental radiological impact caused by the activities of non-nuclear factories, called NORM factories (Naturally Occurring Radioactive Material). These factories are characterized for using, in their production processes, raw materials containing significant levels of natural radionuclides or by the fact that some wastes or by-products can be rich in natural radionuclides. The processing of these materials can expose workers to radiation levels above the natural background.

The present study was carried out in a NORM factory devoted to the production of phosphoric acid by the wet process sited in the city of Huelva, where the sedimentary phosphate rock is dissolved by adding diluted sulphuric acid (60%) generating an exothermic reaction at around 70 ºC, producing the suspension of a solid waste called phosphogypsum (PG) (Rutherford et al, 1994), and a liquid fraction of phosphoric acid (PA), usually with 27% in P_2O_5. These plants started operating in 1965 and were closed at the end of the year 2010, up to that date, they were the greatest producers of phosphoric acid in the European Union, processing annually more than two million metric tons of phosphate rock (PR).

This industry mainly used Moroccan sedimentary phosphate rock containing ^{238}U-series radionuclides with activity concentrations around 1.5 kBq kg^{-1} (Pérez Moreno, 2005 and Bolívar et al, 2009a). However, historically they treated phosphate ores from other geographical areas, such as, for example, Kola Peninsula, containing ^{238}U-series radionuclides with activity concentrations below 100 Bq kg^{-1}, and with similar activity concentrations of ^{232}Th-series isotopes (Pérez-Moreno, 2005). The main difference among both types of rocks was their respective origins: Morocco ore is a sedimentary rock (fluorapatite, $Ca_5(PO_4)_3F$), while Kola ore is an igneous rock ($3Ca_3(PO_4)_2CaF_2$). The differences in geological origins lead to very different radionuclide contents (Bolívar et al, 2009b).

Moreover, it is important to note that in the PA production process the radioactive equilibrium originally present in phosphate rock undergoes a selective fractionation (Bolívar et al, 2009a). In this sense, most of the radionuclides contained in the raw material are dissolved in the first step of sulphuric acid attack, and then they are distributed into phosphoric acid (final product) and phosphogypsum, according to the chemical behavior of each element. Thus, in the conditions of the industrial chemical process (oxidizing conditions), the uranium is very soluble as U (VI) (uranyl-ion UO_2^{2+}) (Markovic et al., 1988), explaining this fact that majority of U (more than) 80% of the uranium originally contained in the raw material remains in the phosphoric acid (liquid fraction). On the other hand, lead sulphate is highly insoluble, precipitating together with calcium sulphate (among other elements of the group II, for example barium and radium sulphates) and polonium, remaining more than 90% of Pb, Ra and Po originally present in the phosphate rock associated to the phosphogypsum waste (Bolívar et al, 1993; Bolívar et al, 1998, Pérez-Moreno et al., 2018). Average activity concentrations of ^{226}Ra, ^{210}Pb and ^{210}Po around 600 Bq kg^{-1} were found in the PG generated in these factories (Más et al, 2006), although with a wide variability.

A complete description of the phosphoric acid industrial process used in the plant of Huelva can be consulted in the previous manuscript (Bolívar et al., 2009a). In short, this process consists of four main stages: (1) grinding, (2) digestion, (3) filtration (concentration), and (4) washing (Figure 1).

FIGURE 1

The process starts with the grinding of phosphate rock (where 90% of this ore is broken down to sizes below 150 μm), continuing with a digestion process, in which raw materials is mixed with diluted sulphuric acid (60%) at around 70 ºC. In the digestion process, a "pulp" containing phosphoric acid in dissolution and a solid waste fraction (phosphogypsum, PG) are formed. The generated pulp is then subjected to a filtration step, where the “phosphoric acid” (liquid phase containing about 27% P_2O_5), and “phosphogypsum” (solid phase) are separated by vacuum filtration of the "pulp" coming from the attack (digestion) step. During the filtration step, for every ton of pure P_2O_5 produced, about 4.5-5tons of phosphogypsum are generated. Then, the solid fraction obtained, mainly composed by PG, is subjected to three washing steps to recover the remaining P_2O_5 from this fraction. The final PG has about 1% of P_2O_5 present insoluble form (around 0.5%) and structural form (around 0.5%), which comes from un-digested PR. Finally, the produced phosphoric acid is stored and “aged” in big tanks (called “decanters”), where oversaturated salts precipitate with an original fine particulate material, forming sludge at the bottom of the decanters at room temperature.

Taking into account the previous exposed facts, the main objective of the present study was to carry out a physicochemical and radioactive characterization of the main materials involved in the production of phosphoric acid by the wet process, in order to understand the mechanisms through which the different elements and radionuclides contained in the ore remain in the

obtained materials and in the generated scales throughout the industrial process. This information is necessary for operators and maintenance personnel involved in clean-up and waste management operations.

2. Materials and methods

2.1 Materials and sampling

After a thorough study of the production steps of phosphoric acid plants, the most significant and representative samples of the entire industrial activity were selected. A description of the samples used in this study and full details can be found in Table 1 and Figure 1. The characterization of the main materials involved in the industrial process were carried out, in order to locate and identify the so-called "hot spots", or points of potential accumulation of radionuclides, which can produce a radiological risk to the plant operators. In addition, the knowledge of these points could be of interest to carry out a future decommissioning operations.

The sampling was carried out in two areas: **a)** *Zone 1*: Phosphoric acid production plant; **b)** *Zone 2*: Deposits of active phosphogypsum.

Each solid sample was dried at 95 ºC until constant weight was reached, and then they were all grinded. Samples [PU], [DS] and [TS] did not dry completely at this temperature; therefore, they were calcined at 350 ºC.

2.2 Methods for physical and chemical characterization

2.2.1 Techniques based on X-ray

2.2.1.1 X-Ray Diffraction (XRD)

The mineralogical studies were carried out by applying the X-ray diffraction technique (XRD). In particular, they were carried out by applying the powder diffraction method in a Bruker diffractometer (model D8 Advance), using Cu Kα radiation filtered by a Ni film and excited with 30 mA of intensity and 40 kV of tension. The mineralogical quantification of the samples was carried out using Bruker's EVA software with internal database. It is worth mentioning that this technique is only valid for detecting crystalline compounds.

2.2.1.2 X-ray Fluorescence (XRF)

The major elements were measured using X-ray fluorescence (XRF) with a Bruker S4 Pioneer system, which had the following characteristics: 4 kW, front window and anode of Rh, five analyzing crystals (LIF200, Ge, PET, OVO55 and OVOC), and two X-ray detectors. This technique requires the samples to be as homogeneous as possible. There are two ways of preparing the samples: as pearls, or as pressed pills. In our case, they were all prepared as pressed pills, taking 6 g of dry sample with 2.4 cm^3 agglutinative Elvacite® dissolved in acetone. The mixture was homogenized in an agate mortar and introduced in the press, maintaining a pressure of 150 bars for 10 seconds, after which the pill was removed.

2.2.1.3 Scanning electron microscopy (SEM) with X-ray microanalysis

The morphology and microstructure of the samples were studied using an environmental scanning electron microscope QUANTA Fei-200, which allows obtaining three-dimensional images of the surface of a solid sample in nanometers (nm) and micrometers (μm). The equipment also provides a semi-quantitative analysis of the surface of interest by energy dispersive spectroscopy (EDS). After the microscopy analysis, a mineralogy database was used to determine the mineralogy according to the obtained composition.

147 The samples were previously subjected to a metallization process with carbon using
148 equipment EMITECH K-550X. The process involved coating the sample with a carbon layer
149 to make it conductive and observable through the electron microscope.

150 The spatial distribution of elements in the samples was obtained by a scanning electron
151 microprobe (Electron Probe Microanalyzer - EPMA) JEOL JXA-8200 model with four
152 wavelength-dispersive X-rays spectrometers (WDS) and energy-dispersive X-rays
153 spectrometer (EDS). This equipment allows identifying elements and determine their relative
154 proportions. An initial analysis involves the generation of an X-ray spectrum of the entire
155 scanning area of the image, which creates elemental highresolution maps. The image is
156 produced by a progressive scanning of the selected sample surface by the electron beam.

157 *2.2.2 Chemical analysis*

158 Trace elements were determined by Inductively Coupled Plasma Mass Spectrometry (ICP-
159 MS). The samples were digested in Savillex digestion vessels with hydrofluoric, nitric and
160 perchloric acid. Hydrofluoric acid is used to remove silica and release chemicals such as ions.
161 Nitric acid is an oxidant that prevents the volatilization of certain elements and perchloric acid
162 is responsible for removing the remaining hydrofluoric acid that may have precipitated as
163 fluoride. The right amount of perchloric acid was added, as too much potassium perchlorate
164 may form a highly insoluble material that can mask the metallic elements. The amounts used
165 were 7 mL, 8 mL and 7 mL of nitric, hydrofluoric and perchloric acid, respectively. All
166 samples were evaporated on a hot plate. After digestion, the final aliquot was reduced to a 2%
167 solution in nitric acid with Milli-Q water for ICP-MS analysis.

168 *2.2.3 Laser granulometry measurements*

169 Granulometry analyses were carried out using the Mastersize 2000 APA 2000 model
170 (©Malvern Instruments Ltd). For an accurate granulometric measurement, a representative

amount of each sample was placed in water for 24 hours to achieve a high level of disintegration of the original matrix. For a correct homogenization of the matrix, each sample was then introduced into a magnetic separator at a constant speed of 700 rotations per minute. Aliquots were collected using the Mastersize 2000 system for their analysis.

2.2.4 Radiometric measuring methods; alpha and gamma spectrometry

The radioactive characterization of the samples was performed by applying two independent techniques: gamma-ray and alpha-particle spectrometry. Gamma measurements were carried out using a gamma spectrometry system equipped with a XtRa coaxial germanium detector (Canberra), with 38% relative efficiency, and FWHM of 0.95 keV at the 122 keV line of ^{57}Co and 1.9 keV at the 1333 keV line of ^{60}Co. The whole procedure of calibration of this gamma spectrometry system is described elsewhere (Mantero et al., 2015). The radionuclides measured by gamma spectrometry were ^{228}Th, Ra-isotopes and ^{40}K.

Po, Th- and U-isotopes activity concentrations were determined by alpha-particle spectrometry in aliquots of the homogenized samples. For the determination of these isotopes, a sequential well-established radiochemical method was applied (Oliveira and Carvalho, 2006) in order to put the radio-elements in dissolution, and then they were isolated and electrodeposited onto stainless steel discs to obtain very thick radioactive sources. The ^{210}Po was obtained by self-deposition on silver discs. The discs were counted by using an EG&G Ortec alpha spectrometry system equipped with ion-implanted silicon detectors.

2.2.5 Dosimetric analysis

Extensive dosimetric sampling was performed through the facilities of the industrial complex, including the areas or locations where the samples were collected. For it, a radiation monitor UMo model LB 123 was used. The “Universal Monitor" (UMo), manufactured by Berthold, is a monitor designed specifically for low dose rates. It is equipped with a probe certified by the

Deutsches Institut für Normunge.V. (the German Institute for Standardization), which works on proportional mode and allows the measurement of both dose rate and integrated dose

2.2.6 Thermogravimetric analysis

In the thermal gravimetric analysis (TGA-DTG) and differential thermal analysis (DTA),a TG-851E 11 SDTA Mettler thermo balance was used, coupled to an equipment of mass spectrometry (MS): Pffeifer Thermostar. This equipment allows determining the composition of the gases from the thermo gravimetric experiment. The operating conditions used were: 25 ºC to 1000 ºC with a heating rate of 10 ºC min^{-1} in inert atmosphere of N_2 with a flow of 50 ml min^{-1}.

2.3 Estimation of internal doses by aerosol inhalation

The assessment of the internal doses by aerosol inhalation has been performed for the samples with higher activity concentration of natural radionuclides (MO), (IS), (ES) and (PG), based on the International Atomic Energy Agency (IAEA) criteria and values (IAEA, 1999, 2004 and 2014) which in turn derive from the International Commission on Radiological Protection (ICRP), notably ICRP Publication 119 (2012) (ICRP, 2011). In this regard, we can define the particulate matter concentration values which would represent an annual committed dose for workers due to inhalation of particulate matter of 1 mSv/y as:

$$\boldsymbol{P = E_j /(Cj \cdot h_j \cdot T \cdot B)} \qquad \text{Eq 1}$$

where,

- $\boldsymbol{P}$ = aerosol concentration in air (kg m^{-3}).
- $\boldsymbol{E_j}$ = annual committed dose received by an individual due to particulate matter inhalation (limits 1 mSv·y^{-1} for public).

- $\mathbf{C_j}$ = concentration of the "j" radionuclide in the particulate matter ($Bq \cdot kg^{-1}$), see Table 2.
- $\boldsymbol{h_j}$ = Dose coefficient for inhalation of the "j" radionuclide ($Sv \cdot Bq^{-1}$). Data values/ assumptions are applied base on the European Union published reference standards (Directive 2003/88/EC), Table S1 (supplementary material). In addition, the most conservative coefficient of the activity median aerodynamic diameter (AMAD),1µm, was chosen.
- $\boldsymbol{T}$ = occupancy factor ($h \cdot y^{-1}$), calculated as a highly conservative assumption in that it represents the maximum working hours permitted by a worker under the EU Directive (Directive 2003/88/EC). 8 hours per day x 250 days per year = 2000 h.
- $\boldsymbol{B}$ = inhalation rate ($m^3 \cdot h^{-1}$) have been assumed for an adult individual engaged in an average level of physical activity = 1.5 $m^3 \cdot h^{-1}$. (ICRP 66, 1994).

3. Results and discussion

3.1. Granulometry

The size distribution in the different studied raw materials was very homogeneous, showing that 90% of the particles were smaller than 150 microns, which is the optimal grain size to carry out the acid digestion step of the process.

FIGURE 2

The grain size distribution of the intermediate materials depends on the origin of each material (Table 1). The [PU] and [DS] samples showed concentrations of 13.5 ± 0.3% and 12.0 ± 0.8%, respectively, for particle sizes below 4 µm (clays). These percentages were considerably higher for sizes between 4 and 63 µm (silts), with 85.5 ± 1.4% and 84.8 ± 0.8%, respectively. There was also a residual fraction of particles larger than 63 µm (sand) in both samples .On the other hand, [TS] and [IS] samples showed a silt distribution of around 85%

241 and certain percentages of particles larger than 500 µm. These particles can be aggregates of
242 particles obtained in the thickening process. Thus, it is clear that the grain particle sizes of
243 these samples are similar, which may indicate that their generation processes could be slightly
244 similar from the granulometric point of view.

245 The [ES] (external scales of the phosphogypsum deposit) sample showed a different grain
246 size distribution (Figure 2), with 52% of lime and 42% of sand, which could be due to the
247 agglomeration of particles in the overflows of the tanks.

248 Finally, the grain size distribution of phosphogypsum samples was different. Fresh
249 phosphogypsum [PG1] had a grain size smaller than that of [PG2], with a concentration of
250 around 85% under 63 µm, while [PG2] showed similar percentages in the lime and sand
251 zones. In this case, the origin of the sample is crucial: [PG1] is "fresh" phosphogypsum
252 directly from the factory and [PG2] is deep phosphogypsum taken from the deposits (1 m
253 deep from surface).

254 **3.2 Mineralogical composition**

255 Fluorapatite, $Ca_5(PO_4)_3F$, is the main mineral component present in phosphate rock of both
256 igneous (Kola [KO]) and sedimentary (Morocco [MO] and Togo [TO]) origin (Rutherford et
257 al, 1994).[MO] and [TO] have a higher content of carbonates, fluorides and metals, such as
258 iron and aluminum, and often contain organic compounds, since their origin is associated with
259 materials derived from living beings (Becker, 1989).

260 Marine sedimentary phosphate, [MO], is used in many factories in Spain and Morocco. The
261 generic formula of the ore used for the manufacture of phosphoric acid is $Ca_{10}(PO_4)_6F_2$, since
262 it was formed by the precipitation of calcium phosphate dissolved in the seawater when deep
263 cold phosphate-rich waters reached the Atlantic Ocean surface and their temperature
264 increased (Busntyski, 1964; McConnel, 1965; Bromely, 1967). Thus, according to our

results, the following species were observed: fluorapatite, $Ca_5(PO_4)_3F$, calcite ($CaCO_3$), and quartz (SiO_2). This composition agrees with those published by other authors (Rentería-Villalobos et al, 2010).

Regarding the intermediate products, the results obtained for the pulp sample [PU], which was taken from the reactor tanks where the phosphate rock is digested by adding diluted sulphuric acid (60%), show that the crystalline phase corresponds to anhydrite ($CaSO_4$), since this one was calcined at 350 ºC, losing the water of its crystalline structure.

The sludge taken from the acid decanter, [DS], was formed by material decanted in this tank from very fine suspended solids that passed through the filter used in the separation of acid-PG, or by suspended particles formed by co-precipitation during the interval time that phosphoric acid is stored in these tanks. As was described in the previous section on the granulometric analysis, the crystalline phase of this sludge corresponds to the very fine particles of anhydrite ($CaSO_4$) and highly insoluble alkaline fluorosilicates, such as malladrite (Na_2SiF_6).

The external scales [ES] from the phosphogypsum tanks, where the gypsum is pumped toward the rafts, are basically composed of gypsum, sulphate calcium dihydrate ($CaSO_4{\cdot}2H_2O$), and alkaline fluorosilicates, such as malladrite (Na_2SiF_6), with traces of quartz (SiO_2). In the same way, the [IS] sample (internal scale taken from inside a phosphoric acid production pipe) is mainly composed of heklaite ($KNaSiF_6$) and malladrite (Na_2SiF_6), with traces of gypsum ($CaSO_4{\cdot}2H_2O$). Heklaite in mineralogical form only appears in the [IS] sample, as it is more insoluble than malladrite in acidic media (Fayret et al, 2006), especially in sulfuric media.

Finally, the two phosphogypsum samples analyzed, [PG1] and [PG2], are in agreement with the expected results, with gypsum ($CaSO_4{\cdot}2H_2O$) being the main mineral present in their

289 composition. Both samples showed the same crystalline composition, with gypsum as the
290 main phase composition of the phosphogypsum waste.

291 The presence of bassanite ($CaSO_4 \cdot 0.5H_2O$) is explained by water loss through evaporation at
292 95 °C (Ostroff, 1964; Guan et al, 2009). This was observed when the phosphogypsum
293 samples, which were previously dried in an oven at 95 °C for 24 h, were analyzed using XRD.
294 In fact, the crystalline composition showed a significant change, indicating that calcium
295 sulfate hemihydrate and calcium sulfate dihydrate can coexist (Rentería-Villalobos, et al
296 2010).

297 **3.3 Major elements**

298 Table S2 of supplementary material shows the concentrations of the major elements
299 determined by XRF for the studied samples. The raw material samples had similar
300 concentrations of F and SiO_2 (about 4% and 2.3%, respectively), and significant amounts of
301 P_2O_5 (27%), and CaO (52%), as is expected for the ores used in the production of phosphoric
302 acid (PA), and in agreement with the mineralogy previously discussed in section 3.1.
303 Concentrations of Na, Al, K and Fe were also observed in non-negligible amounts.

304 With regard to intermediate products, the pulp [PU] had a significant percentage of P_2O_5
305 (15%), since the solid fraction in the digestion step is a mixture of PG+PA. The mineralogy
306 results support this conclusion, as the largest phase found was anhydrite ($CaSO_4$), with SO_3
307 and CaO values of 31% and 34%, respectively, and a remnant of quartz (0.4% SiO_2).

308 Both the decanter sludge [DS] and thickener sludge [TS] samples contained high values of
309 phosphorus (15.5% and 27.5% of P_2O_5, respectively), indicating that a fraction of them was
310 probably formed by the remaining phosphoric acid and particulate matter co-precipitated
311 during the storage of phosphoric acid inside these storing tanks. There were also significant
312 amounts of sulfate given as SO_3 (30.2% and 20.4%, respectively), and CaO (31.9 % and 21%,

313 respectively), ratifying that a significant fraction of these sludge samples was formed by very
314 fine particles of phosphogypsum.

315 The scale samples ([IS] and [ES]) presented high contents of F (56.5 % and 26.3%,
316 respectively), which probably came from precipitated salts found in the phosphoric acid, since
317 alkali fluorosilicates (for example, potassium and sodium fluorosilicate) are highly insoluble.
318 In this sense, high concentrations of SiO_2 (24 % and 9.9%, respectively) and Na_2O (16.5 %
319 and 5.8%, respectively) in the scales samples were found. [IS] shows the highest
320 concentrations of both Na and K, and very low values of Ca and SO_3, indicating that this scale
321 was mainly formed by highly insoluble salts of alkali fluorosilicates, such as heklaite, as we
322 can see in the XRD section. On the other hand, the [ES] sample shows significant values of
323 SO_3 (41%) and CaO (25%) due to the presence of calcium sulfate in the mineral composition.
324 It is interesting to remember that this sample was taken from the outer surface of the tank,
325 where the phosphogypsum is pumped into the ponds.

326 Finally, the concentration of both SO_3 and CaO in the phosphogypsum samples ([PG1] and
327 [PG2]) indicates that more than 90% of these samples corresponds to calcium sulphate.
328 Moreover, important impurities of P_2O_5 (~ 1 %), Al_2O_3 (~ 0.2 %), Na_2O (~ 0.2 %), SiO_2 (~ 1
329 %) and F (~ 2 %) were found in PG2 (see Table S2). The very low pH (< 2) of PG2, which
330 was stored in the piles, is mainly due to their remaining phosphoric acid content (around 1%),
331 enabling the leaching of both these ones and other pollutants into their surrounding
332 environment.

333 In the phosphogypsum samples, SiO_2 can be found as quartz, which, together with Al_2O_3 and
334 Na_2O and/or K_2O, could indicate the presence of clay minerals ($Al_2O_3 \cdot 2SiO_2 \cdot H_2O$) (Arocena
335 et al, 1995). These results are in agreement with those found ones by other authors for similar
336 phosphogypsums (Martín, 1999). Lastly, as was also expected, higher concentrations of P_2O_5

were found in the fresh phosphogypsum sample ([PG1]), since older phosphogypsum ([PG2]) stored for long periods is subjected to longer leaching processes.

3.4 Trace elements

Table S3 of supplementary material shows the obtained results for trace elements in intermediate products and waste generated in the process, which are compared with the raw materials used in the process and the global average concentration of uncontaminated soils (Rudnick and Gao, 2003).

Igneous phosphate rock ([KO]) is rich in Ba and rare earth elements, such as La, compared to sedimentary ores ([TO] and [MO]) (Da Conceicao, 2006; Barros de Oliveira, 2007). For example, the concentration of Ba in [KO] was 633 mg kg^{-1}, which is significantly higher than those obtained in the two sedimentary raw materials [MO] (97 mg kg^{-1}), and [TO] (47 mg kg^{-1}). Furthermore, the concentrations of heavy metals in the igneous sample given by Da Conceicao (Da Conceicao, 2006) (Cd, 4 mg kg^{-1}; Cr, 70 mg kg^{-1}; Ci, 96 mg kg^{-1}; Ni, 117 mg kg^{-1};Pb, 44 mg kg^{-1}; Zn, 326 mg kg^{-1}), are higher than those found in this work. Some authors (Martín et al, 1999; Pérez-López et al, 2007) also published concentrations of heavy metals in samples of sedimentary phosphate rock from Morocco, which are in agreement with those of the [PR] sample of this study (see Table S3).

In the intermediate products, the [TS] sample showed high concentrations for most of the analyzed trace elements (Cd, Cr, Ni, Sr, Y, Zn, and Th). It is also worth mentioning the high concentration of Y(1370 mg kg^{-1}), La(702 mg kg^{-1}) and U (154 mg kg^{-1}) found in [TS]. This fact can be explained by the origin of this sludge: solid complex salts and very small particles of PG, which are formed in the concentrated phosphoric acid step, where these particles are highly enriched in trace elements during their formation.

Regarding the scale samples [ES] and [IS], Table S3 shows that the concentrations of most of the trace elements (As, Mn, Sr, Cu, Pb, Ni and Cr) are higher in [ES] than in [IS]. It is important to remember that [ES] are scales from the surface of the phosphogypsum deposit, where they are pumped into the PG piles. In this sense, previous studies (Wang, 2001; Gunasekaran and Chauhan, 2004) have demonstrated that the wet process of phosphoric acid preparation generates severe corrosion problems in containers and that the corrosion of the stainless steel vessel should also be considered as an additional source of several elements like Cr, Cu, Ni, and Zn (Beddow et al., 2006).

In phosphogypsum samples, most trace elements have similar or lower values than those reported by other authors in phosphogypsum derived from sedimentary phosphate rock (Rentería-Villalobos et al, 2010). Potential contaminants such as Cd present high concentrations, up to 20-fold higher than that of a typical unperturbed soil. Finally, Table S3 shows similar trace element concentrations for both phosphogypsum samples, which can be explained by the fact that trace elements tend to gather and rest in the matrix of phosphogypsum that is already settled.

3.5. Microestructural Analysis

In order to deeply study the generated scales in the phosphoric acid production process, scanning electron microcopy was carried out in both scale samples [ES] and [IS], Figures S2 and S3 of suplementary material.

Figure S1 shows that the main composition of the [IS] sample is heklaite ($KNaSiF_6$) (point 5), malladrite (Na_2SiF_6) (points 1 and 2) and gypsum ($CaSO_4 \cdot 2H_2O$) (points 3 and 4), showing the typical morphology of gypsum particles, similar to other industrial wastes rich in gypsum (Gazquez et al, 2009). This results are in accordance with the mineralogical studies (XRD) and major elements (XRF).

A representative SEM image, corresponding to the [ES] samples analyzed in this work, is shown in Figure S2, where it is possible to observe that the external scales sample is composed of particles of very heterogeneous sizes, in agreement with the granulometry results. Moreover, the composition shows quartz (point 1), gypsum (point 2) and malladrite (point3), as was expected, taking into account the mineralogical composition.

3.6 Termogravimetric analysis

In this section, a calorimetric study was carried out in order to characterize and measure the behavior of these materials when exposed to temperatures up to 1000 ºC by means of thermogravimetric analysis (TGA).

3.6.1. External scales (ES)

Figure 3 shows the TG and DTG curves for the external scales [ES] waste, in which DTG was calculated by the first derivative of the mass loss as a function of the temperature (rate of mass changes with respect to the temperature T). This analysis shows four thermal events at 110 ºC (with a maximum weight/temperature change ratio at 149 ºC), 500 ºC (with a maximum at 592 ºC), 700 ºC (with a maximum at 752 ºC) and finally 825 ºC (with a maximum at 847 ºC). The first peak on the DTG curve detected a loss of water, which is characteristic at this temperature, as it corresponds to the loss of structural water in the phosphogypsum. Taking into account the loss of water (13.1%), we can estimate that the gypsum content of the sample is 62.6% (with 14.6% of Ca and 11.6% of S). Considering the concentration of the major elements shown in Table S2, we can assert that not all the sulphur content in the sample is in the gypsum form.

FIGURE 3

The second thermal event observed (500 ºC) corresponds to the decomposition of malladrite (Na_2SiF_6) identified by XRD. This mineral decomposes at 500-600 ºC, according to the next chemical reaction:

Na_2SiF_6 (s) → 2NaF (s) + SiF_4 (g)

Taking into account the mass loss at this point (19%) see Figure 3, we can estimate that [ES] contains 34.3% of malladrite (F = 20.8%, Si = 5.10%, Na= 8.39%) as was expected, considering the results obtained by XRF.

The third peak observed in Figure 3 is compatible with the decomposition of carbonates at about 700ºC (Demir et al, 2003). On the other hand, according to previous studies (Tõnsuaadu et al., 2012) the fourth thermal event can be compatible with decomposition of hydroxyapatite ($Ca_5(PO_4)_3(OH)$ not identify previously by XRD usually associated with fluorapatite), which takes place within a range of 800‑900 ºC (maximum at 830ºC), which matches our results (Figure 3).

The SDTA curve reveals that all the events that took place were endothermic and caused by the decomposition of the different chemical species contained in the sample.

3.6.2 Internal Scales (IS)

The analysis of the [IS] showed six thermal events with a maximum weight/temperature change ratio at 104 °C, 200 °C, 455 °C, 535 °C,720 °C and 836 °C, see Figure 4 .The first two peaks are compatible with the loss of the chemically bound water. In this case, the water not only came from the gypsum, but also from other minor hydrated compounds not identified previously by XRD.

FIGURE 4

The most important thermal event occurred at 720 ºC. This peak corresponds to the decomposition of heklaite and malladrite. Taking into account the concentration of the major elements shown in Table S2 (13.5%, 11.2%, 12.2% and 56.5% for K, Si, Na and F, respectively), we can estimate their percentages. Assuming that all the potassium contained in the sample remained associated with heklaite (containing by stoichiometry 19.1% of K), we can estimate that the percentage of heklaite mineral is around 70%, while that of malladrite is around 30%, approximately. These quantities are in agreement with the mass loss at this temperature. In this case, heklaite mineral is decomposed as follows:

$KNaSiF_6 \rightarrow NaK\ (s) + KF(s) + SiF_4(g)$

In this case, the SDTA curve also reveals that all the events that took place were endothermic and caused by the decomposition of the different chemical species contained in the sample.

3.7. Radioactive characterization

Table 2 shows the radionuclide activity concentrations of the raw material samples, intermediate products and phosphogypsum samples. Regarding the raw materials, the activity concentration of ^{238}U was variable, ranging between 70 Bq kg^{-1} in the [KO] sample and 1200-1600 Bq kg^{-1} in the raw materials with sedimentary origin, thereby corroborating the fact that phosphates used at Huelva factories from sedimentary origins ([TO] and [MO]) show higher uranium content than the igneous phosphate from Kola ([KO]) (Habashi, 1980; Cavalcanti-Canut, et al 2008; Bolívar et al., 2009a).

With respect to the concentration of ^{232}Th, this was similar in samples [KO] and [TO], about 80 Bq kg^{-1}, with a 4-fold decrease in [MO] (20 Bq kg^{-1}), which is similar to that of undisturbed soil. On the other hand, ^{40}K concentrations were very low (around 40 Bq kg^{-1}), which is one order of magnitude lower than the average of potassium for typical soils from Spain (range, 100-1000 Bq kg^{-1}; average, 600 Bq kg^{-1}).

In general remarks, it can be seen that in the three raw materials analyzed and for each natural radioactive series (^{238}U and ^{232}Th), the radionuclides are in secular equilibrium. Finally, taking into account that the raw material used in the factory of Huelva is the phosphate rock coming from morocco [MO], the activity concentrations of elements included in the Th series (^{232}Th, ^{228}Ra and ^{228}Th) are lower than those corresponding to the unperturbed soil, 35 Bq kg^{-1} (UNSCEAR, 2000). Therefore, we can assert that, from the radiological point of view, the relevance of the Th series versus the U series is very limited.

During the phosphoric acid production process, the radioactive equilibrium is broken. Thus, uranium mainly remains in phosphoric acid (under oxidizing conditions, at up to 90%), while most of the radium is transferred into phosphogypsum and solid materials (Gorecka and Gorecki, 1984; Rutherford et al, 1994; Bolívar et al, 1995; Bolívar et al., 2009a). The obtained results are in agreement with this behavior. Thus, the activity concentration of ^{226}Ra and ^{210}Po are higher than the activity concentration of ^{238}U in solid materials, except in the PR.

Regarding intermediate products, uranium has a tendency to be concentrated in samples with higher contents of P_2O_5. Thus, the thickener sludge [TS] has 1210 Bq kg^{-1} of ^{238}U, compared to the 1000, 735, 245 and 228 Bq kg^{-1} measured in the pulp [PU], decanter sludge [DS] and both scales [IS] and [ES] respectively (samples with lower concentrations of P_2O_5 shown in Table S2).

Uranium is highly soluble, presenting a very high linear correlation with P_2O_5 concentrations, as expected from a previous work (Bolivar et al, 2009a). In fact, Figure S3 of supplementary materials shows a linear relation between the concentrations of these elements, suggesting that uranium travels along the PA production process bound to phosphoric acid (soluble fraction), following Equation 2:

$$^{238}U\ (Bq\ kg^{-1}) = (121 \pm 61) + (42.7 \pm 4.5)P_2O_5\ ,R^2 = 0.919 \qquad [Eq.\ 2]$$

The previous fitting has a determination coefficient (R^2) of 0.919, and the constant is not statistically significant. Regarding ^{230}Th, this radionuclide seems to be associated with the solid fraction of phosphogypsum (in agreement with most studies, Bolívar et al, 2009a; Bolívar et al, 1995). Nevertheless, in the samples of intermediate products, this radionuclide seems to have a strong tendency to bind the soluble fraction too. Thus, in the sludge sample, for example, the concentrations of ^{230}Th were similar to those of ^{238}U. This indicates that thorium is also highly soluble in phosphoric acid and that the thorium fraction linked to the acid varies depending on its concentration.

On the other hand, the highest concentrations of ^{226}Ra were found in the sludge samples ([DS] and [TS], 1140 and 2300 Bq kg^{-1}, respectively similar to previous studies (Bolivar et al., 2009a)), in [IS] (around 9000 Bq kg^{-1}), and in [ES] (4250 Bq kg^{-1}). These results indicate that the highest enrichments of radium are associated with the fine textured material that either flows in suspension in the PA liquid fraction or is formed when the concentrated PA is produced.

In general, ^{210}Po tends to "travel" throughout the industrial process adhered to the solid phases (Bolívar et al., 2009a), although, in general, its concentrations are lower than those of ^{226}Ra, except in [ES] sample, see Table 2. This is possibly due to the fact that polonium tends to co-precipitate with gypsum to a lesser extent than radium. The explanation may lie in the fact that polonium is slightly more soluble in phosphoric acid than radium, and, therefore, some of it remains in the P_2O_5 still contained in the gypsum (3000 Bq kg^{-1} of ^{210}Po [TS] compared to 800-1200 Bq kg^{-1} measured in samples of phosphogypsum).

The concentrations of ^{40}K, in general, are very low in relation to unperturbed soils, as expected, except for the sludge and scale samples. The [IS] sample contained about 5000 Bq kg^{-1}and [DS] showed over 300 Bq kg^{-1}, which are compatible with the K_2O concentration obtained by XRF, with Concentration Factors (CFs) of 140 and 9, respectively, calculated in

503 relation to the [PR] concentration (CF = C_X/C_{PR}). These results are probably related to the
504 "special" mineralogy of these scales, which contain high levels of alkalifluorosilicates (highly
505 insoluble).
506 The ratio of $^{230}Th/^{232}Th$ in [PR] is the same (≈ 80), and the low values of ^{232}Th in all products
507 confirm that [MO] is usually employed throughout the industrial process. On the other hand,
508 it is important to note that the $^{226}Ra/^{238}U$ ratio in the mineral is in secular equilibrium, ratio 1;
509 however, in the scale samples an important enrichment takes place, showing values of 18.6
510 for [ES] and rising significantly to 37 in the [IS] sample.

511 **3.8 Radiological risks**

512 Table 3 shows the maximum dose rate above background recorded in these areas. Analyzing
513 the results obtained, and in comparison with the activity concentration values present in each
514 sample (Table 2), it can be verified that the "shielding" effect plays a relevant role. Thus, for
515 example, samples that were collected outdoors such as phosphogypsum [PG1] and [PG2] or
516 raw materials [MO], have associated dose rate values according to their natural radiation
517 content. On the other hand, samples with a higher natural radioactivity content such as [DS]
518 and [TS] samples have lower dose rate values associated. This fact is due to the shielding
519 effect exerted by the containers/vessels/pipes where these samples have been generated. The
520 clearest case is found in the [IS] sample (scale inside a pipe). This sample shows, as a whole,
521 the highest activity concentration values of all the samples analyzed, and however the
522 measured dose rate value is not the highest. This shielding effect does not occur, for example,
523 in the [ES] sample, since it is an external scale, and that is why it has the highest associated
524 dose rate value.

525 For exposure to externally ionizing radiation to be less than 1 mSv y^{-1}, the dose rate value
526 must be less than 0.5 μSv h^{-1} for a workday of 2000 h y^{-1}. Taking this dose rate value as a
527 reference, it can be verified that only the value of 1 mSv y^{-1} could be exceeded in the areas
528 associated with the presence of scales [IS and ES], therefore the occupancy factor in the

maintenance operations of the equipment/facilities should be taken into account. Thus, is recommended do not exceed 600 and 1400 hours per year in the zone of [ES] and [IS], respectively.

On the other hand, particulate matter concentration values (P, calculated using Eq 1) which would represent an annual committed dose for workers due to inhalation of particulate matter of 1 $mSv \cdot y^{-1}$ are 3.27, 6.68, 2.97 and 8.15 $mg \cdot m^{-3}$ for [MO], [IS], [ES] and [PG1] samples.

These values demonstrate that to reach the value of 1 $mSv \cdot y^{-1}$, it would be necessary, in the worst cases, to experience dust concentrations under operational conditions several times higher or similar than Occupational Exposure Limits (OELs) for Respirable dust (3 $mg \cdot m^{-3}$) (ITC/2585/2007 Order). For that reason, will be necessary to take precautions, by using the dust mask for working procedures involving dust.

The result associated with the PG1 sample indicates that it is the sample with the lowest radiological risk. In addition, the moisture content of this material on average is over 15%, so the generation of dust would not be relevant. In relation to the both scales analyzed (IS and ES), the ES sample has the highest associated risk. As with phosphogypsum, the scales are normally in a wet state. Furthermore, it is important to remember that the estimates have been made taking into account an occupancy factor of 2000 hours per year, which is far from realistic, since this type of materials would only be contacted during decommissioning or maintenance operations of short duration.

Lastly, despite the fact that the raw material (OM in this case) shows one of the lowest values of particulate matter concentration which would represent an annual committed dose for workers due to inhalation of particulate matter of 1 mSv y-1, the radiological risk associated with the inhalation path can be important. The dust generation is much more likely in operations such as milling and transportation once it is milled through the facility. However,

553 the control of dust generation and the use of masks can reduce the radiological risk associated
554 with this material and the path of exposure to non-relevant values.

555 **4.CONCLUSIONS**

556 This work was aimed at the physical-chemical and radioactive characterization of the main
557 materials involved in the production process of phosphoric acid by wet sulfate: raw materials,
558 intermediate materials (sludges and scales) and wastes. This characterization allowed testing
559 and evaluating the degree of fractionation of different elements and compounds analyzed in
560 the main stages of the industrial process, proving to be useful to the maintenance personnel of
561 the factory.

562 The main conclusion of this study was that the high content of natural radionuclides in some
563 inner pipe scales, mud and outer incrustations, have to be taken into account in the
564 radiological protection of the workers involved in the clean-up and waste management
565 operations.

566 In addition, the partials conclusions drawn from this study are the following:

567 1.- The radioactive results indicate that the main raw material used in the manufacturing
568 process, i.e., phosphate rock from Morocco, is a NORM material, since it contains significant
569 concentrations of thorium and uranium, around 50-fold higher than those of undisturbed soil.

570 2.- Due to concentration processes, both the external ([ES]) and internal scales ([IS]) obtained
571 in the phosphoric acid factory are enriched in natural radionuclides, mainly by ^{226}Ra and
572 ^{210}Po.

573 2.1 The external scales ([ES]) presents activity concentrations of ^{226}Ra and ^{210}Po
574 around 4 and 6 Bq g^{-1}, respectively, which are around 150 -fold higher than the concentrations
575 found it in unperturbed soils.

2.2 The internal scales ([IS]) showed high concentrations of ^{226}Ra (9 Bq g^{-1}) and ^{40}K (5 Bq g^{-1}), fact explained by the high contents in heklaite ($KNaSiF_6$).

2.3.- The sludge samples ([TS] and [DS]), showed high activity concentrations (3 Bq g^{-1}) around 100 times higher than those of unperturbed soils for radionuclides from uranium series, and high values of P_2O_5 and significant amounts of SO_3 and CaO, explained by their origin.

3.- Phosphogypsum samples show a higher activity concentration for ^{226}Ra and around 1 Bq g^{-1}, with gypsum ($CaSO_4 \cdot 2H_2O$) as the main mineralogical phase (> 95%).

4.-The granulometric results of intermediate products show that practically 90% of the particles are below 63 μm in the samples of pulp sludge (decanted and thickened), as well as in the inner scales. On the other hand, external scales show a greater grain size, with 40% in the sandy area. This fine granulometry could have significant implication in the radiological doses receives by the workers.

5. The shielding effect exerted by the containers/vessels/pipes has an essential role in the external dose measured in the intermediate products. In this regard, the external scale analyzed has by far the highest associated dose rate value, but not the highest radionuclide activity concentration. The internal dose of the natural radionuclides with higher activity concentrations have been assessed, obtaining that if the maximum particulate matter concentration established in the Spanish regulation is verified, and taking into account the most conservative scenario, the annual limit of 1 mSv y^{-1} is not exceeded.

Funding information: This research was partially supported by the Spanish Government Department of Science and Technology (MINECO) through the project "Fluxes of Radionuclides Emitted by the Phosphogypsum Piles Located at Huelva; Assessment of the

Dispersion, Radiological Risks and Remediation Proposals" (Ref. CTM 2015-68628-R),), and the project of the Regional Government of Andalusia called “Basic processes regulating the fractionations and enrichments of natural radionuclides under acid mine drainage conditions” (Ref.: UHU-1255876).

5.- REFERENCES

Arocena J.M., Rutherford P.M, Dudas M.J., 1995. Heterogeneous distribution of trace elements and fluorine in phosphogypsum by-product. Sci Total Environ.162, 149-160.

Barros de Oliveira S.M., Cardoso da Silva P.S., Paci Mazzilli B., Teixeira Favaro D.I., Saueia C.H., 2007. Rare earth elements as tracers of sediment contamination by phosphogypsum in the Santos estuary, southern Brazil. Appl Geochem. 22, 837-850.

Becker P., 1989. Phosphates and Phosphoric Acid: raw materials, technology, and economics of the wet process, ENSCS Strasbourg, France.

Beddow H., Black S., Read D., 2006. Naturally occurring radioactive material (NORM) from a former phosphoric acid processing plant. J. Environ. Radioactiv. 86, 289-312.

Bolívar J.P., García-Tenorio R. y Más J.L., 1998. Radioactivity in Phosphogypsum in the South-west of Spain. Radiat Prot Dosim, 76, 185-189.

Bolívar J.P., García-Tenorio R., García-Leon M. 1995. Fluxes and distribution of natural radionuclides in the production and use of fertilizers. Appl Radiat Isol. 46 (6/7), 717-718.

Bolívar J.P., Martín J.E., Garcıía-Tenorio R., Perez-Moreno J.P., Mas J.L. 2009a. Behaviour and fluxes of natural radionuclides in the production process of a phosphoric acid plant. Applied Radiation and Isotopes 67, 345–356.

622 Bolívar J.P., Martínez Aguirre A. y García-Tenorio R., 1993. Radioactivity involved in the
623 production of fertilizers: radioecological impact. In Proceedings European Meeting on
624 Chemical Industry and Environment 311-320.

625 Bolívar J.P., Pérez-Moreno J.P., Mas J.L., Martín J.E., San Miguel E.G., García-Tenorio R.,
626 2009b. External radiation assessment in a wet phosphoric acid production plant. Appl Radiat
627 Isot 67, 1930-1938.

628 Bromley R.G., 1967. Marine phosphorites as depth indicators". Marine Geology. 5**,** 503–509.

629 Busntyski G. I., 1964. On shallow water origin of phosphorite deposits. Developments in
630 sedimentology. 1, 62-70.

631 Cavalcanti-Canut M.M, Feliciano-Jacomino V.M, Bratwit K., Magalhaães-Gomes A.,
632 Yohsida M.I. 2008. Microstructural analyses of phosphogypsum generated by Brazilian
633 fertilizer industries. Mater Charact. 59, (4) 365-373.

634 Da Conceicao F.T., Bonotto D.M., 2006. Radionuclides, heavy metals and fluorine incidence
635 at Tapira phosphate rocks, and their industrial (by) products. Environ Pollut. 139, 232-243.

636 Demir F., Donmez B., Okur H., Sevim F., 2003. Calcination kinetic of magnesite from
637 thermogravimetric data. Inst. Chem. Eng. Trans. I Chem E 81, Part A.

638 Directive 2003/88/EC of the European Parliament and of the Council of 4 November 2003
639 concerning certain aspects of the organisation of working time, http://eur-lex.europa.eu/legal-
640 content/EN/ALL/?uri=CELEX:32003L0088

641 Frayret J., Castetbon A., Trouve G., Potin-Gautier M., 2006. Solubility of $(NH_4)_2SiF_6$, K_2SiF_6
642 and Na_2SiF_6 in acidic solutions. Chemical Physics Letters 427, 356–364.

643 Gázquez, M. J., Bolívar, J. P, Garcia-Tenorio, R.;Vaca, F., 2009. Physicochemical
644 characterization of raw materials and co-products from the titanium dioxide industry. J.
645 Hazard. Mater. 166 (2), 1429-1440.

646 Gorecka H., Gorecki H. 1984. Determination of uranium in phosphogypsum. Talanta 31 (12),
647 1115-1117.

648 Guan B.,Yang L., Wu Z., Zhen Z., Ma X., Ye Q., 2009. Preparation of a calcium sulfate
649 hemihydrates from FGD gypsum in K, Mg-containing concentrated $CaCl_2$ solution under mild
650 conditions. Fuel. 88, 1286-1293.

651 Gunasekaran G., Chauhan L.R., 2004. Eco friendly inhibitor for corrosion inhibition of mild
652 steel in phosphoric acid medium. Electrochimica Acta 49, 4387-4395.

653 IAEA 2014 Radiation Protection and Safety of Radiation Sources: International Basic Safety
654 Standards, General Safety Requirements, Safety Standards Series No. GSR Part 3. European
655 commission, food and agriculture organization of the united nations, international atomic
656 energy agency, international labour organization, OECD nuclear energy agency, pan
657 American health organization, united nations environment programme, world health
658 organization http://www-pub.iaea.org/MTCD/publications/PDF/Pub1578_web-57265295.pdf

659 IAEA 2004, International Atomic Energy Agency.Methods for Assessing Occupational
660 Radiation Doses Due to Intakes of Radionuclides, Safety Reports Series, 37, Vienna.

661 IAEA 1999, International Atomic Energy Agency, International Labour Office. Assessment
662 of Occupational Exposure Due to Intakes of Radionuclides, Safety Guide, SAFETY
663 STANDARDS SERIES No. RS-G-1.2, Vienna (1999).

664 ICRP, 1994. International Commission On Radiological Protection, Human Respiratory Tract
665 Model for Radiological Protection ICRP Publication 66, Ann. ICRP 24 (1-3), 1994.

ICRP, 2011. International Commission On Radiological Protection, Compendium of Dose Coefficients based on ICRP Publication 60, ICRP PUBLICATION 119, Approved by the Commission in October 2011, (2012).

ITC / 2585/2007, of 30 August 2007, Supplementary Technical Instruction 2.0.02 "Protection of workers against dust, in relation to silicosis, in the extractive industries", of the General Regulation of Mining Safety Rules.

Mantero J. , Gázquez M.J. , Hurtado S. , Bolívar J.P., García-Tenorio R. 2015. Application of gamma-ray spectrometry in a NORM industry for its radiometrical characterization. Radiation Physics and Chemistry, 116, 78-81.

Markovic M., Pavkovic N. and Neven D. Pavkovic. 1988.. Precipitation of $NH_4U0_2P0_4 \cdot 3H_20$- Solubility and Structural Comparison with Alkali Uranyl(2 +) Phosphates. J Res Nat Bur Stand. *93*(4), 557–563.

Martín J.E., García-Tenorio R., Respaldiza M.A., Ontalba M.A., Bolívar J.P., Da Silva M.F., 1999. TTPIXE analysis of phosphate rocks and phosphogypsum. Appl Radiat Isot. 50, 445-449.

Más J.L., Borrego E., Martín J.E., Bolívar J.P., Vaca F., Pérez Moreno J.P., 2006. An assay of the effect of preliminary restoration task applied to a large TENORM wastes disposal in the south-west of Spain. Sci Total Environ 364, 55-66.

McCoNNELL, D., 1965.Precipitation of phosphates in sea water. Econ Geol. 60, 1059 - 1062.

Oliveira J.M., Carvalho F.P., 2006. Sequential extraction procedure for determination of uranium, thorium, radium, lead and polonium radionuclides by alpha spectrometry in environmental samples". Czech J of Phys, 56, 545-555.

689 Ostroff A.G., 1964. Conversion of gypsum to anhydrite in aqueous salt solutions", Geochim.
690 Cosmochim Acta. 28, 1363-1372.

691 Pérez Moreno J.P. 2005. Natural radionuclides in the fertilizers Industry. Ph.D. Thesis,
692 University of Seville (in Spanish).

693 Pérez Moreno J.P., San Miguel E. G., Bolívar J. P., Aguado J. L. 2002. A comprehensive
694 calibration method of Ge detector for low level spectrometry measurement. Nucl Instrum
695 Meth A, 491 (1-2), 152-162.

696 Pérez-Moreno S.M., Gázquez M.J., Pérez-López R., Bolívar J.P. 2018. Validation of the BCR
697 sequential extraction procedure for natural radionuclides. Chemosphere. 198, 397-408

698 Pérez-López R., Álvarez-Valero A.M., Nieto J.M., 2007. Changes in mobility of toxic
699 elements during the production of phosphoric acid in the fertilizer industry of Huelva (SW
700 Spain) and environmental impact of phosphogypsum wastes. J. Hazard. Mater. 148 (3), 745-
701 750.

702 Rentería-Villalobos M., Vioque I., Mantero J., Manjón G., 2010. Radiological, chemical and
703 morphological characterizations of phosphate rock and phosphogypsum from phosphoric acid
704 factories in SW Spain. J. Hazard. Mater. 181, 193-203.

705 Rudnick R.L., Gao S., 2003. Composition of the Continental Crust. Treatise of Geochemistry.
706 Elsevier, vol 3, The Crust, 2003.1-64.

707 Rutherford P.M., Dudas M.J., Samek R.A., 1994. Environmental impacts of phosphogypsum.
708 Sci Total Environ 149, 1-38.

709 Tõnsuaadu, K., Gross, K. A., Pluduma, L., & Veiderma, M. (2012). A review on the thermal
710 stability of calcium apatites. J Therm Anal Calorim, 110(2), 647–659.

711 United Nations Scientific Committee on the effects of Atomis Radiation (UNSCEAR), Report
712 of the United Nations Scientific Committee on the effects of Atomis Radiation, United
713 Nations, New York, 2000.

714 Wang, L., 2001. Evaluation of 2-mercaptobenzimidazole as corrosion inhibitor for mild steel
715 in phosphoric acid. Corrosion Science 43, 2281-2289.

716

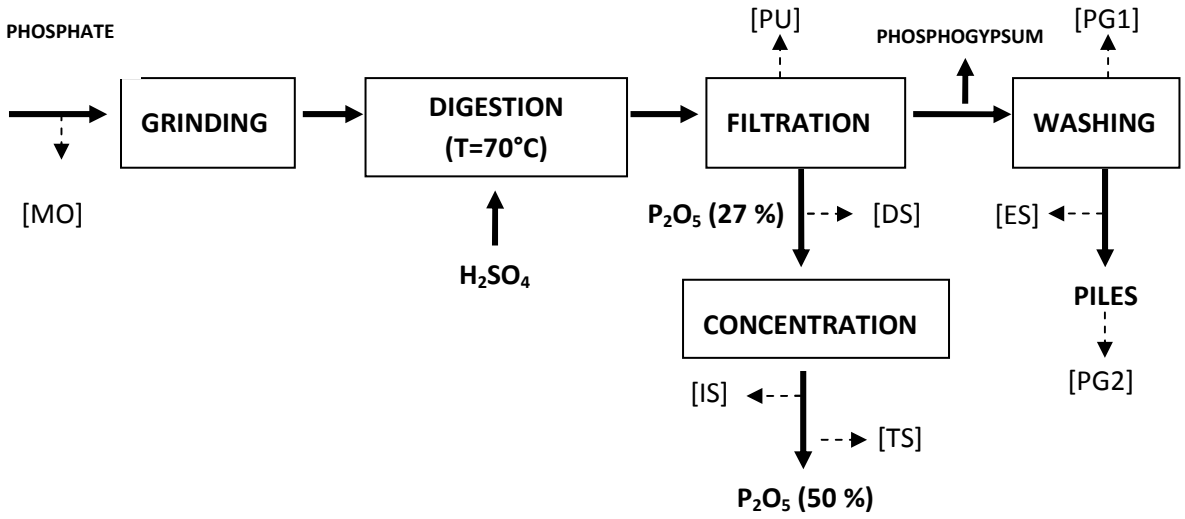

Figure 1. Scheme of the manufacturing process of phosphoric acid. Collected samples in brackets.

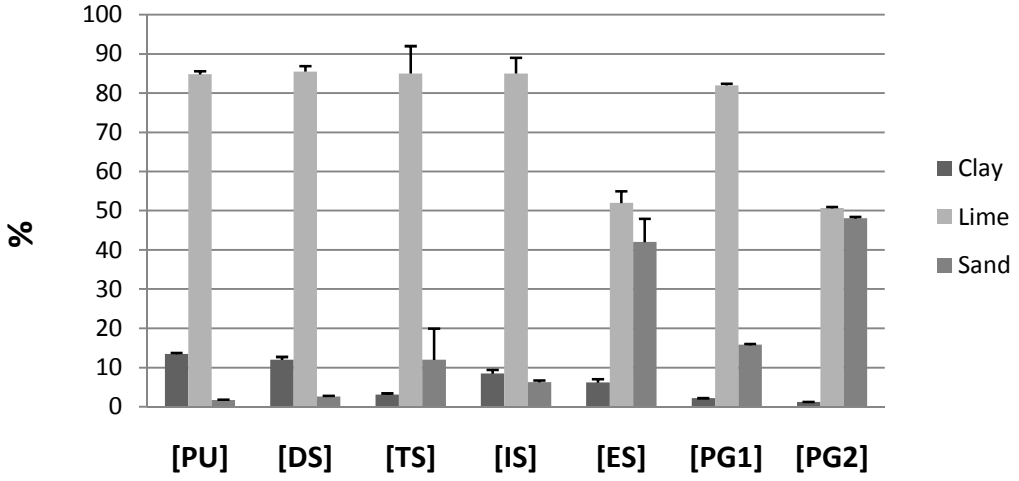

Figure 2. Average grain-size composition (%) of intermediate samples and phosphogypsum samples**.** Clay < 4 µm, lime < 63 µm and sand < 2000µm.

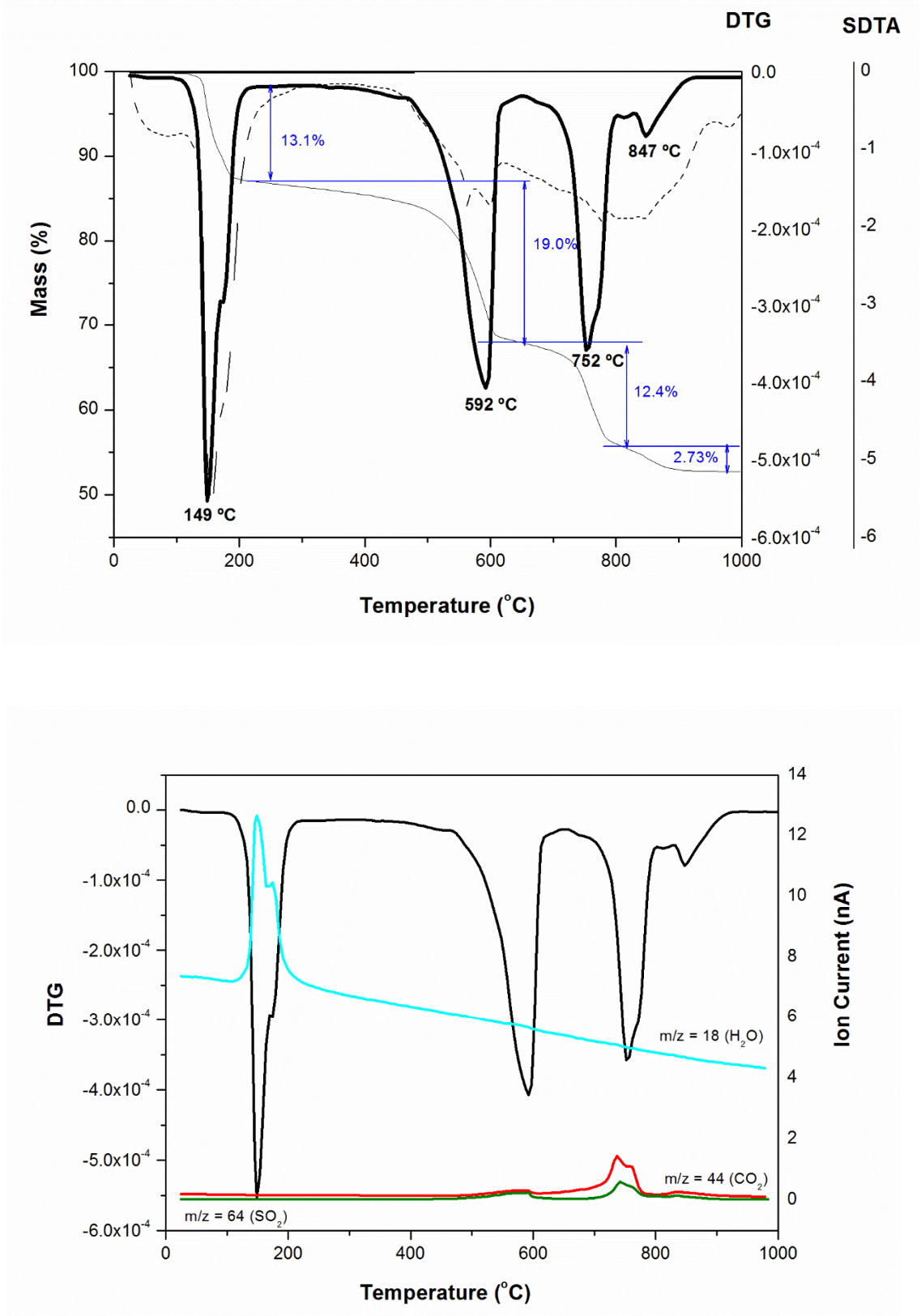

Figure 3. TG-DTG-SDTA-MS analysis of the [ES] sample.

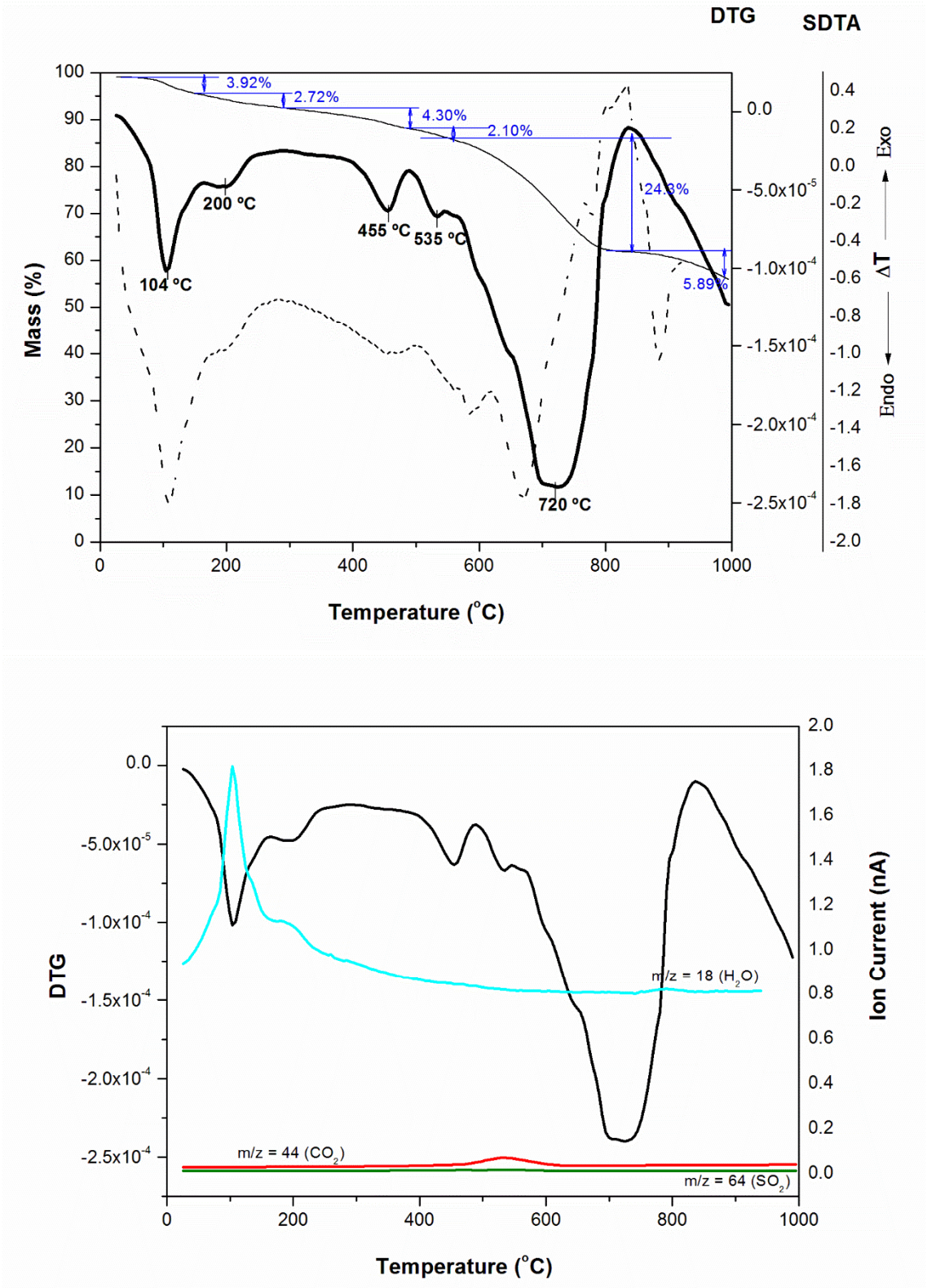

Figure 4. TG-DTG-SDTA-MS analysis of the [IS] sample.

Table 1. Descriptive summary of the collected samples.

CLASSIFICATION	CODE	SAMPLE	DESCRIPTION
RAW MATERIALS	**KO**	Kola	Phosphate rock from Kola Peninsula (igneous origin, deposit of Oblast, northern Russia)
	TO	Togo	Phosphate rock from Togolese Republic (sedimentary origin).
	MO	Morocco	Phosphate rock from Morocco (sedimentary origin). Un-milled fraction stored in silos
INTERMEDIATE PRODUCTS FROM THE INDUSTRIAL PROCESS	**PU**	Pulp	Solid fraction obtained by filtration of the pulp from the acid attack step.
	DS	Decanter Sludge	Solid fraction coming from clarifier or decanter (27 %)
	TS	Thickener Sludge	Solid fraction coming from sludge thickener (50 %)
	IS	Scale	Scale taken from inside a phosphoric acid production pipe
	ES	External Scale	External scales from the phosphogypsum deposit where this is pumped into the PG piles.
FINAL WASTEOF THE PROCESS	**PG1**	Phosphogypsum	Fresh phosphogypsum taken just before it is pumped to the piles.
	PG2	Phosphogypsum	Deep phosphogypsum taken from the stacks (1 m below surface)

Table 2. Activity concentration (Bq/kg) for radioelements of interest. Uncertainties of 1σ. ^{210}Po in secular equilibrium with ^{210}Pb

	^{238}U	^{234}U	^{230}Th	^{226}Ra	^{210}Pb (^{210}Po)	^{232}Th	^{228}Th	^{228}Ra	^{40}K	^{230}Th/^{232}Th	^{226}Ra/^{228}Ra	^{226}Ra/^{238}U
[KO]	69.7 ± 2.3	70.6 ± 2.3	70 ± 5	76 ± 5	97 ± 4	88 ± 5	105 ± 7	104 ± 7	54 ± 6	0.80 ± 0.07	0.73 ± 0.07	1.09 ± 0.08
[TO]	1200 ± 30	1200 ± 30	1100 ± 60	1373 ± 80	1240 ± 30	80 ± 7	82 ± 5	90 ± 6	< 48	14 ± 1	15 ± 1	1.14 ± 0.07
[MO]	1610 ± 30	1612 ± 30	1600 ± 70	1770 ± 70	1520 ± 40	20 ± 2	< 7	< 16	36 ± 7	80 ± 9	>110	1.10 ± 0.05
[PU]	991 ± 22	991 ± 22	780 ± 40	700 ± 40	880 ± 30	8 ± 2	< 5	<10	< 34	98 ± 25	>70	0.71 ± 0.04
[DS]	735 ± 17	742 ± 18	880 ± 60	2300 ± 140	1780 ± 40	16 ± 3	< 13	< 27	320 ± 30	55 ± 11	>85	3.1 ± 0.2
[TS]	1210 ± 40	1199 ± 40	2640 ± 90	1140 ± 30	3350 ± 90	30 ± 2	24 ± 5	13 ± 6	96 ± 19	88 ± 7	88 ± 41	0.94 ± 0.04
[IS]	245 ± 16	265 ± 17	1800 ± 50	9000 ± 500	1400 ± 40	19 ± 2	29.5 ± 1.9	85 ± 5	5000 ± 300	95 ± 10	106 ± 9	37 ± 3
[ES]	228 ± 9	217 ± 9	120 ± 6	4250 ± 120	6580 ± 160	3 ± 1	< 9	15.8 ± 1.9	200 ± 16	40 ± 13	260 ± 30	18.6 ± 1.0
[PG1]	86 ± 5	83 ± 4	750 ± 15	1120 ± 70	1150 ± 40	11 ± 4	28.3 ± 2.3	53 ± 4	25 ± 5	70 ± 28	21 ± 2	13.0 ± 1.0
[PG2]	143 ± 3	144 ± 4	510 ± 40	950 ± 60	780 ± 30	17 ± 4	< 4	7.4 ± 0.8	< 23	30 ± 7	128 ± 16	6.6 ± 0.4

Table 3. Maximum dose rate above background associated to the zones where the samples were collected. Background of the area: 0.09 μSv/h. Note: MO was the only raw material present in the facility when the dosimetric sampling was performed.

CODE	ZONE	MAXIMUN DOSE RATE (μSv/h)
MO	Raw materials stacks	0.56
PU	Filtration zone	0.49
DS	Decantation zone	0.26
TS	Concentration zone	0.18
IS	Reaction/filtration zone	0.70
ES	Phosphogypsum pumping tanks	1.60
PG1/PG2	Phosphogypsum stacks	0.25